Noname manuscript No.
(will be inserted by the editor)

Distance from the Nucleus to a Uniformly Random Point in the 0-cell and the Typical Cell of the Poisson-Voronoi Tessellation

Praful D. Mankar · Priyabrata Parida · Harpreet S. Dhillon · Martin Haenggi

Received: date / Accepted: date

Abstract Consider the distances $\tilde{R}_o$ and R_o from the nucleus to a uniformly random point in the 0-cell and the typical cell, respectively, of the d-dimensional Poisson-Voronoi (PV) tessellation. The main objective of this paper is to characterize the exact distributions of $\tilde{R}_o$ and R_o. First, using the well-known relationship between the 0-cell and the typical cell, we show that the random variable $\tilde{R}_o$ is equivalent in distribution to the contact distance of the Poisson point process. Next, we derive a multi-integral expression for the exact distribution of R_o. Further, we derive a closed-form approximate expression for the distribution of R_o, which is the contact distribution with a mean corrected by a factor equal to the ratio of the mean volumes of the 0-cell and the typical cell. An additional outcome of our analysis is a direct proof of the well-known spherical property of the PV cells having a large inball.

Keywords Poisson point process · Poisson-Voronoi tessellation · Typical cell · 0-cell · Distance distribution.

P. D. Mankar, P. Parida and H. S. Dhillon
Wireless@VT, Bradley Department of Electrical and Computer Engineering,
Virginia Tech,
Blacksburg, VA, USA.
E-mail: {prafuldm, pparida, hdhillon}@vt.edu

M. Haenggi
Department of Electrical Engineering,
Department of Applied and Computational Mathematics and Statistics,
University of Notre Dame,
Notre Dame, IN, USA.
E-mail: mhaenggi@nd.edu

Corresponding author: H. S. Dhillon
Email: hdhillon@vt.edu. Phone: +1 (540) 231-2129. Fax: +1 (540) 231-2968.

1 Introduction

Due to its useful mathematical properties, the Poisson point process (PPP) has found many applications in several fields of science and engineering, such as statistical physics, telecommunications, astronomy, biology, metallurgy, and geography, to name a few. Several of these applications specifically focus on the Poisson-Voronoi (PV) tessellation [1], which partitions space into disjoint *cells* whose nuclei are the points of the PPP. There is a rich literature focused on characterizing the statistical properties of the PV tessellation (PVT), such as the distributions of the contact and chord lengths [2], the distributions of the radii of the circumcircle and the incircle of the 0-cell and the typical cell [3], the distribution of the number of edges of the typical cell [4], the limiting shape of the 0-cell and the typical cell [5], the properties of the 3-dimensional PV tessellation [6], and the relationship between the 0-cell and the typical cell [7]. Two very recent examples from statistical physics include the derivation of the first and second moments of the area of the edge-cells of a bounded PV tessellation in [8] and the proof of existence of all the exponential moments for the total edge length of different planar tessellations including PV and Johnson-Mehl tessellations in [9]. Despite this rich history, it is quite surprising to note that the distributions of the distances from the nucleus to uniformly random points in both the 0-cell and the typical cell of the d-dimensional PV tessellation have not yet been investigated, which is the main goal of this paper. Our main result builds on the calculation methods developed in statistical physics to study the temporal evolution of the domain structure of a 2-dimensional PV tessellation in [10].

The motivation behind our investigation comes from wireless networks, where the PPP has been extensively used to model the locations of cell towers (also called base stations) in cellular networks such that the service region of each cell tower is simply the PV cell with the corresponding cell tower at its nucleus [11, 12, 13, 14, 15]. If one assumes mobile users to be distributed uniformly at random in the service region of each cell tower (a popular model used by the wireless networks community), one of the crucial steps towards the performance characterization of this network is to understand the distribution of the distance between a mobile user and its associated cell tower. In the PV tessellation, this corresponds to the distribution of the distance of the nucleus of a PV cell to a point chosen uniformly at random from that cell [16, 17]. Note that while it is sufficient to focus on the 2-dimensional case from the wireless networks perspective, all the mathematical results presented in this paper are for the general d-dimensional case. With this brief introduction, we now formally define the problem of interest for this paper.

Let $\Phi \triangleq \{\mathbf{x}_1, \mathbf{x}_2, \dots\}$ be a homogeneous PPP with intensity λ on $\mathbb{R}^d$. The PV cell with the nucleus at $\mathbf{x} \in \Phi$ is defined as

$$V_{\mathbf{x}} = \{\mathbf{y} \in \mathbb{R}^d \mid \|\mathbf{y} - \mathbf{x}\| \leq \|\mathbf{x}' - \mathbf{y}\|, \ \forall \mathbf{x}' \in \Phi\}, \quad \mathbf{x} \in \Phi. \tag{1}$$

The set $\{V_{\mathbf{x}}\}_{\mathbf{x}\in\Phi}$ is known as the *PVT*. For any (deterministic) $\mathbf{y} \in \mathbb{R}^d$, almost surely there exists a unique nucleus $\mathbf{x} \in \Phi$ such that $\mathbf{y} \in V_{\mathbf{x}}$ [18]. The PV cell

containing the origin o is called the *0-cell* and is denoted by $\tilde{V}_o$. The statistical properties of the *typical cell* can be characterized using Palm theory, which formalizes the notion of conditioning on the presence of a point of a point process at a specific location. Since by Slivnyak's theorem, conditioning on a point is the same as adding a point to a PPP, we consider that the nucleus of the typical cell of the point process $\Phi \cup \{o\}$ is o, which is given by

$$V_o = \{\mathbf{y} \in \mathbb{R}^d \mid \|\mathbf{y}\| \leq \|\mathbf{x} - \mathbf{y}\|, \ \forall \mathbf{x} \in \Phi\}. \tag{2}$$

Now, we define the main random variables of interest for this paper.

Definition 1 Let $\tilde{R}_o$ denote the distance from the nucleus to a uniformly random point in the 0-cell $\tilde{V}_o$.

Definition 2 Let R_o denote the distance from the nucleus to a uniformly random point in the typical cell V_o.

We derive the cumulative distribution function (CDF) of $\tilde{R}_o$ and R_o in Sections 2 and 3, respectively. In Section 2, a closed-form expression for the exact CDF of $\tilde{R}_o$ is derived based on the formula on the relationship between the 0-cell and the typical cell given in [7, 11]. It is well-known that the statistical properties of R_o are hard to characterize for $d > 1$. Before going into the $d > 1$ case, we discuss the case of $d = 1$ in Section 3.1 for which the distribution of R_o is far easier to characterize. In Section 3.2, we present an analytical approach to derive a multi-integral expression for the exact distribution of R_o for $d > 1$ based on the analysis of the temporal evolution of the PV structure presented in [10]. Since this multi-integral expression may be unwieldy for some applications, we also derive a simple closed-form approximation for the CDF of R_o in Section 4. Finally, based on the formulation developed in Section 3, we provide a simpler proof for the well-known spherical nature of the large PV cells in Section 5.

2 Distribution of $\tilde{R}_o$

In this section, we derive a closed-form expression for the CDF of the distance from the nucleus to uniformly random point in the 0-cell $\tilde{V}_o$. It is well-known that the expected volume of the 0-cell is greater than the expected volume of the typical cell. In fact, all the moments of the volume of the 0-cell are known to be greater than the moments of the volume of the typical cell [7]. This is quite intuitive as the origin (or, for that matter, any *fixed* point) is more likely to lie in a bigger cell. The relationship of the distributions of the 0-cell and the typical cell is given by [11, Corollary 4.2.4]

$$\mathbb{E}[f(\tilde{V}_o)] = \lambda \mathbb{E}[\upsilon_d(V_o) f(V_o)], \tag{3}$$

where υ_d is the Lebesgue measure in d-dimensions, and f is a translation-invariant non-negative measurable function on compact sets.[1] We will use this expression along with an appropriately chosen function f to derive the CDF of $\tilde{R}_o$ in Theorem 1. Let $\mathcal{B}_r(\mathbf{x})$ represent the d-dimensional ball of radius r centered at $\mathbf{x}$. Next, we restate a useful result from [19, Lemma 4.2] on the mean volume of $\mathcal{B}_r(o) \cap V_o$, which directly follows from [20].

Lemma 1 *For the homogeneous PPP with intensity λ on $\mathbb{R}^d$, the mean volume of the intersection of the ball $\mathcal{B}_r(o)$ with the typical cell V_o is given by*

$$\mathbb{E}[\upsilon_d(\mathcal{B}_r(o) \cap V_o)] = \frac{1}{\lambda} \left(1 - \exp(-\lambda \kappa_d r^d)\right), \tag{4}$$

where $\kappa_d = \frac{\pi^{\frac{d}{2}}}{\Gamma(\frac{d}{2}+1)}$ is the volume of the unit-radius ball in $\mathbb{R}^d$.

Now, we present the CDF of $\tilde{R}_o$ using the result given in Lemma 1.

Theorem 1 *For the homogeneous PPP with intensity λ on $\mathbb{R}^d$, the CDF of the distance $\tilde{R}_o$ from the nucleus to a uniformly random point in the 0-cell $\tilde{V}_o$ is*

$$F_{\tilde{R}_o}(r) = 1 - \exp\left(-\lambda \kappa_d r^d\right), \quad r \geq 0. \tag{5}$$

Proof Let $\mathbf{x}_o$ represent the nucleus of $\tilde{V}_o$ and let $\mathbf{y}$ represent the uniformly distributed point in $\tilde{V}_o$. We note that the distance $\tilde{R}_o = \|\mathbf{x}_o - \mathbf{y}\|$ is less than r when $\mathbf{y}$ lies in the intersection of the ball $\mathcal{B}_r(\mathbf{x}_o)$ and $\tilde{V}_o$. Therefore, the CDF of $\tilde{R}_o$ can be written as

$$F_{\tilde{R}_o}(r) = \mathbb{P}(\tilde{R}_o \leq r) = \mathbb{E}\left[\frac{\upsilon_d(\mathcal{B}_r(\mathbf{x}_o) \cap \tilde{V}_o)}{\upsilon_d(\tilde{V}_o)}\right].$$

Now, we define the function f of the PV cell $V_{\mathbf{x}}$ as the ratio of the volumes of $\mathcal{B}_r(\mathbf{x}) \cap V_{\mathbf{x}}$ and $V_{\mathbf{x}}$. Thus, we get

$$f(\tilde{V}_o) = \frac{\upsilon_d(\mathcal{B}_r(\mathbf{x}_o) \cap \tilde{V}_o)}{\upsilon_d(\tilde{V}_o)} \quad \text{and} \quad f(V_o) = \frac{\upsilon_d(\mathcal{B}_r(o) \cap V_o)}{\upsilon_d(V_o)}.$$

Inserting this in (3), we obtain the result from Lemma 1. □

Remark 1 Using the void probability, the distribution of the distance between the origin and the nucleus of $\tilde{V}_o$, *say* $\mathbf{x}_o$, can be simply determined as $\mathbb{P}(\|\mathbf{x}_o\| \leq r) = 1 - \exp(-\lambda \kappa_d r^d)$. However, it does not reveal any information about how the origin is distributed in the 0-cell. While one can intuitively expect the origin to be uniformly distributed in $\tilde{V}_o$, there does not appear to be a straightforward way to prove this. Using (3), we have presented a simple construction to establish that the distribution of the origin in $\tilde{V}_o$ is in fact that of a uniformly random point in $\tilde{V}_o$.

[1] Alternatively, RHS of (3) may be written using the Palm measure [11]. However, since we have already defined V_o in (2) by placing the typical point of Φ at o, the Palm notation is not necessary here.

3 Distribution of R_o

We first characterize the CDF of R_o for $d = 1$ where the typical cell is completely characterized by the locations of the nearest points on either side of its nucleus. This allows us to explicitly describe the uniformly distributed point in the typical cell V_o and, in turn, determine the CDF of R_o.

3.1 Distribution of R_o for $d = 1$

Let $\Phi_l \triangleq \{x_1, x_2, \dots\}$ be a homogeneous PPP with intensity λ on $\mathbb{R}$. Let $x \in \Phi_l \cap \mathbb{R}^-$ and $y \in \Phi_l \cap \mathbb{R}^+$ be the left and right neighboring points of the origin (i.e., nucleus of V_o), respectively. Since Φ_l is a PPP, $|x|$ and $|y|$ are i.i.d. random variables that follow an exponential distribution with mean λ^{-1}. Denote by $R_1 = \frac{1}{2}|x|$ and $R_2 = \frac{1}{2}|y|$ the distances to the boundary points of V_o. R_1 and R_2 are also i.i.d. and follow exponential distribution with parameter 2λ. Let $\tilde{R}_1 = \min(R_1, R_2)$ and $\tilde{R}_2 = \max(R_1, R_2)$. The joint probability density function (pdf) of $\tilde{R}_1$ and $\tilde{R}_2$ is

$$f_{\tilde{R}_1,\tilde{R}_2}(r_1, r_2) = 8\lambda^2 \exp\left(-2\lambda\left(r_1 + r_2\right)\right), \quad 0 \le r_1 \le r_2. \tag{6}$$

The distribution of the distance R_o from the nucleus to a uniformly random point in the typical cell V_o conditioned on $\tilde{R}_1$ and $\tilde{R}_2$ is

$$\mathbb{P}(R_o \le r \mid \tilde{R}_1 = r_1, \tilde{R}_2 = r_2) = \begin{cases} \frac{2r}{r_1+r_2}, & 0 \le r \le r_1 \\ \frac{r+r_1}{r_1+r_2}, & r_1 < r \le r_2 \\ 1, & r_2 < r. \end{cases} \tag{7}$$

By deconditioning the above expression with respect to the joint distribution of $\tilde{R}_1$ and $\tilde{R}_2$, the CDF of R_o is presented in the following theorem.

Theorem 2 *For the homogeneous PPP with intensity λ on $\mathbb{R}$, the CDF of the distance R_o from the nucleus to a uniformly random point in the typical cell V_o is*

$$F_{R_o}(r) = 1 - \exp(-2\lambda r) + 2\lambda r \exp(-2\lambda r) - 4\lambda^2 r^2 \mathtt{E}_1(2\lambda r), \quad r > 0, \tag{8}$$

where $\mathtt{E}_1(z) = \int_z^\infty \frac{1}{t}\exp(-t)\mathrm{d}t$ is the exponential integral function.

Proof Using the expression for the conditional CDF of R_o given in (7) and the joint pdf of $\tilde{R}_1$ and $\tilde{R}_2$ given in (6), the CDF of R_o can be written as

$$\begin{aligned} F_{R_o}(r) = &\int_0^r \int_0^{r_2} 8\lambda^2 \exp(-2\lambda(r_1 + r_2))\mathrm{d}r_1\mathrm{d}r_2 \\ &+ \int_r^\infty \int_0^r \frac{r + r_1}{r_1 + r_2} 8\lambda^2 \exp(-2\lambda(r_1 + r_2))\mathrm{d}r_1\mathrm{d}r_2 \\ &+ \int_r^\infty \int_r^{r_2} \frac{2r}{r_1 + r_2} 8\lambda^2 \exp(-2\lambda(r_1 + r_2))\mathrm{d}r_1\mathrm{d}r_2. \end{aligned} \tag{9}$$

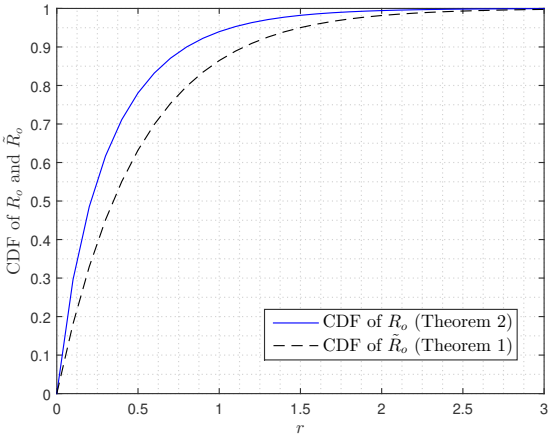

Fig. 1 CDF of R_o and $\tilde{R}_o$ for a unit-intensity Poisson point process for $d = 1$.

Next, the substitution of $r_1+r_2 = y$ and the application of exponential integral function yields the result. The calculations are tedious but straightforward. □

In Fig. 1, we provide the plots for the CDFs of R_o and $\tilde{R}_o$. From the figure, it can be seen that the distance $\tilde{R}_o$ stochastically dominates the distance R_o. In Section 4, we will demonstrate that this difference between the distributions of $\tilde{R}_o$ and R_o diminishes with increasing d.

3.2 Distribution of R_o for $d > 1$

Similar to the distribution of R_o for $d = 1$ being derived by conditioning on the nuclei of the neighboring PV cells in Section 3.1, here we derive the distribution of R_o for $d > 1$ by conditioning on the points in a ball centered at the origin such that it includes the nuclei of all neighboring PV cells of V_o. We refer to the conditional positions of points in the ball as the *domain configuration*. The domain configuration enables the characterization of the shape and size of the PV cell V_o which will be useful in the evaluation of the conditional distribution of R_o. A similar construction is presented in [10, 21] to study the temporal evolution of the volume of the domain size and free boundary distributions for a PV transformation[1] for $d = \{1, 2, 3\}$[2]. In the following subsection, we define the domain configuration and discuss its use for the conditional PV cell characterization.

[2] The simultaneously growing sets of randomly distributed nuclei (realized through PPP) at equal isotropic rate are referred to as the *PV transformation*. These sets eventually transform into the PV cells.

3.2.1 Domain Configuration

Definition 3 For $\ell > 0$, we define the set $\mathcal{C}_\ell^k$ as the set of k points with polar coordinates $(l_i, \boldsymbol{\theta}_i)$ such that

$$\mathcal{C}_\ell^k \equiv \frac{1}{2}\{\Phi \cap \mathcal{B}_{2\ell}(o) \mid \Phi(\mathcal{B}_{2\ell}(o)) = k\}. \tag{10}$$

where l_i is the radial coordinate and $\boldsymbol{\theta}_i = [\theta_{1i}, \ldots, \theta_{(d-1)i}]$ are the angular coordinates.

The point $\tilde{\mathbf{x}}_i \triangleq (l_i, \boldsymbol{\theta}_i) \in \mathcal{C}_\ell^k$ bisects the line segment joining o and $\mathbf{x}_i \in \Phi \cap \mathcal{B}_{2\ell}(o)$. Thus, for a given $\mathbf{x}_i \triangleq (2l_i, \boldsymbol{\theta}_i) \in \Phi \cap \mathcal{B}_{2\ell}(o)$, we have corresponding $\tilde{\mathbf{x}}_i \in \mathcal{C}_\ell^k$ with polar coordinates $(l_i, \boldsymbol{\theta}_i)$. By construction, $l_i \in [0, \ell]$, $\theta_{(d-1)i} \in [0, 2\pi)$ and $\theta_{1i}, \ldots, \theta_{(d-2)i} \in [0, \pi]$. Henceforth, the set $\mathcal{C}_\ell^k$ is referred to as the *domain configuration*. Since Φ is a PPP, conditioned on $\Phi(\mathcal{B}_{2\ell}(o)) = k$, the points $\mathbf{x}_i \in \Phi \cap \mathcal{B}_{2\ell}(o)$, for $i \in \{1, \ldots, k\}$, are distributed uniformly at random independently of each other in $\mathcal{B}_{2\ell}(o)$. Consequently, the k points $\{\tilde{\mathbf{x}}_i\}_{i=1}^k$ forming the domain configuration $\mathcal{C}_\ell^k$ are also distributed uniformly at random independently of each other in $\mathcal{B}_\ell(o)$. Using this fact, we can express the pdf of the domain configuration as done next.

The differential volume element in d dimensions in polar coordinates is

$$\Delta = v^{d-1} \sin^{d-2}(\alpha_1) \ldots \sin(\alpha_{d-2}) \mathrm{d}v \mathrm{d}\alpha_1 \ldots \mathrm{d}\alpha_{d-1}.$$

Thus, the probability that a point distributed uniformly at random in $\mathcal{B}_\ell(o)$ lies in an infinitesimal region with volume Δ_i such that $v_i \leq \ell$ is equal to $\frac{\Delta_i}{\kappa_d \ell^d}$. Now, we obtain the pdf of the configuration $\mathcal{C}_\ell^k$ as

$$\begin{aligned}
&\mathbb{P}((l_1, \boldsymbol{\theta}_1) \in \Delta_1, \ldots, (l_k, \boldsymbol{\theta}_k) \in \Delta_k; \ell) \overset{(a)}{=} \prod_{i=1}^k \mathbb{P}((l_i, \boldsymbol{\theta}_i) \in \Delta_i) \\
&\overset{(b)}{=} \prod_{i=1}^k \frac{1}{\kappa_d \ell^d} v_i^{d-1} \sin^{d-2}(\alpha_{1i}) \ldots \sin(\alpha_{(d-2)i}) \mathrm{d}v_i \mathrm{d}\alpha_{1i} \ldots \mathrm{d}\alpha_{(d-1)i},
\end{aligned} \tag{11}$$

for $0 \leq v_i \leq \ell$, where (a) follows from the independence of the elements of $\mathcal{C}_\ell^k$ and (b) follows from the uniform distribution of elements of $\mathcal{C}_\ell^k$ in $\mathcal{B}_\ell(o)$.

3.2.2 Connections with the Typical Cell

For an empty domain configuration $\mathcal{C}_\ell^0$, $\mathcal{B}_\ell(o)$ is contained in the typical cell V_o. However, a non-empty domain configuration, i.e., $\mathcal{C}_\ell^k$ for $k > 0$, contains the mid-points of the chords of $\mathcal{B}_\ell(o)$ formed by the intersection of the edges of typical cell V_o with $\mathcal{B}_\ell(o)$. In addition, the line segments connecting these mid-points to the origin are perpendicular to the corresponding edges. Therefore, the domain configuration provides useful information about the structure of V_o. We denote by $V_o(\mathcal{C}_\ell^k)$ the typical cell conditioned on the domain configuration $\mathcal{C}_\ell^k$. As $k \to \infty$, it is easy to see that $V_o(\mathcal{C}_\ell^k)$ becomes deterministic. However,

for any finite k, $V_o(\mathcal{C}_\ell^k)$ is in general random because some of its edges may be defined by points of Φ lying outside $\mathcal{B}_{2\ell}(o)$. That said, conditioning on $\mathcal{C}_\ell^k$ is sufficient to uniquely determine the intersection of $V_o(\mathcal{C}_\ell^k)$ and the ball $\mathcal{B}_\ell(o)$. Fig. 2 illustrates the intersection of the $\mathcal{B}_\ell(o)$ with the cell $V_o(\mathcal{C}_\ell^3)$ for $d = 2$.

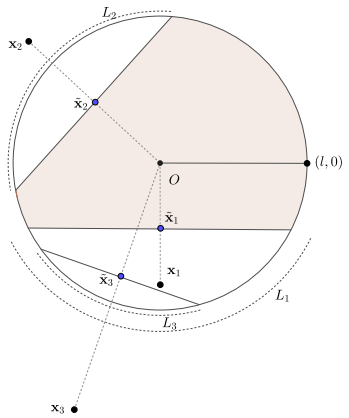

Fig. 2 Illustration of $V_o(\mathcal{C}_\ell^3) \cap \mathcal{B}_\ell(o)$ for $d = 2$.

Let us define $H_{\mathbf{x}}$ as the half-space formed by the points in $\mathbb{R}^d$ that are closer to the point $\mathbf{x} \in \Phi$ than the origin, i.e.,

$$H_{\mathbf{x}} \triangleq \{\mathbf{y} \in \mathbb{R}^d \mid \|\mathbf{y} - \mathbf{x}\| < \|\mathbf{y}\|\}. \tag{12}$$

Now, we denote by $L_i(\ell)$ the surface (in $d-1$ dimensions) of the spherical cap of $\mathcal{B}_\ell(o)$ such that

$$L_i(\ell) \triangleq H_{\mathbf{x}_i} \cap \partial\mathcal{B}_\ell(o), \tag{13}$$

where $\partial\mathcal{B}_\ell(o)$ is the boundary of $\mathcal{B}_\ell(o)$. An illustration of the formation of the $L_i(\ell)$ is presented in Fig. 2 for $d = 2$. Now, since $\{\tilde{\mathbf{x}}_i\}_{i=1}^k$ are distributed uniformly at random in $\mathcal{B}_\ell(o)$ independently of each other, the corresponding surfaces of the spherical caps $\{L_i(\ell)\}_{i=1}^k$ have i.i.d. surface areas[3] and are placed uniformly at random on $\partial\mathcal{B}_\ell(o)$. We will now use this construction to derive the distribution of R_o.

3.2.3 Distance Distribution

For a given domain configuration $\mathcal{C}_\ell^k$, we define

$$g_k(r; \mathcal{C}_\ell^k) = v_d(V_o(\mathcal{C}_\ell^k) \cap \mathcal{B}_r(o)), \tag{14}$$

for $0 \le r \le \ell$, as the volume of the intersection of $\mathcal{B}_r(o)$ and cell $V_o(\mathcal{C}_\ell^k)$. As discussed before, $V_o(\mathcal{C}_\ell^k)$ is the typical cell conditioned on $\mathcal{C}_\ell^k$.

[3] The surface area in this case is the Lebesgue measure in $d-1$ dimensions.

Definition 4 Let R_ℓ denote the distance from the nucleus of V_o (i.e., the origin) to a uniformly random point in $V_o \cap \mathcal{B}_\ell(o)$.

The first main goal is to characterize the CDF of R_o given by

$$F_{R_o}(z) = \lim_{\ell \to \infty} \mathbb{P}(R_\ell \leq z). \tag{15}$$

This conditional CDF of R_ℓ can be expressed as

$$F_{R_\ell}(r; \mathcal{C}_\ell^k) = \frac{\upsilon_d(V_o(\mathcal{C}_\ell^k) \cap \mathcal{B}_r(o))}{\upsilon_d(V_o(\mathcal{C}_\ell^k) \cap \mathcal{B}_\ell(o))} = \frac{g_k(r; \mathcal{C}_\ell^k)}{g_k(\ell; \mathcal{C}_\ell^k)}, \quad 0 \leq r \leq \ell. \tag{16}$$

Fig. 3 provides the visual interpretation of $g_k(r, \mathcal{C}_\ell^k)$ and $g_k(l, \mathcal{C}_\ell^k)$ for the typical cell for $d = 2$. The region $g_k(r; \mathcal{C}_\ell^k)$ is shaded in green and the region $g_k(\ell; \mathcal{C}_\ell^k)$ is shaded in brown for $k = 5$. Naturally, our next goal is to characterize $g_k(r; \mathcal{C}_\ell^k)$ for a given r. For this we will use $\{L_i(r)\}_{i=1}^k$ which is defined in (13).

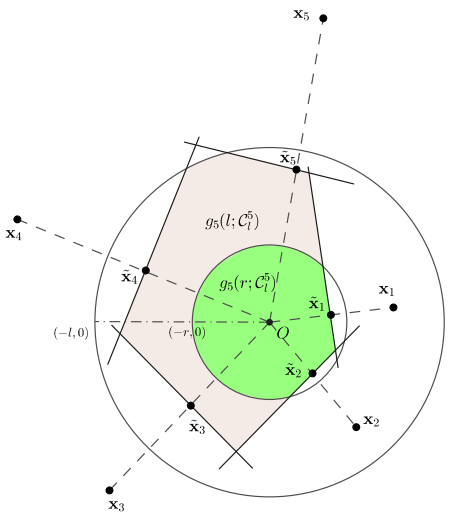

Fig. 3 Illustration of $g_5(r; \mathcal{C}_\ell^5)$ and $g_5(\ell; \mathcal{C}_\ell^5)$ for $d = 2$.

Define the index set $\mathcal{I}(r)$ as the collection of indices i for which $l_i \leq r$. This set points to the collection of the points $\tilde{\mathbf{x}}_i$ of the domain configuration that lie inside $\mathcal{B}_r(o)$. The union $\cup_{i \in \mathcal{I}(r)} L_i(r)$ represents the portion of $\partial \mathcal{B}_r(o)$ that is outside the typical cell $V_o(\mathcal{C}_\ell^k)$. This can be seen easily from Fig. 3 for $d = 2$, where the arcs on $\mathcal{B}_r(o)$ corresponding to $\tilde{\mathbf{x}}_1 \equiv (l_1, \theta_1)$ and $\tilde{\mathbf{x}}_2 \equiv (l_2, \theta_2)$ do not lie in the cell. Using this insight, we will explicitly characterize the portion of $\partial \mathcal{B}_r(o)$ that lies in $V_o(\mathcal{C}_\ell^k)$, which will then be used to derive the CDF of R_ℓ. This evaluation requires a careful consideration of the overlaps between the surfaces of the spherical caps $\{L_i(r)\}_{i \in \mathcal{I}(r)}$.

Let $\mathbf{y} \triangleq (r, \boldsymbol{\alpha})$ be the point on the $\partial\mathcal{B}_r(o)$, where $\boldsymbol{\alpha} = [\alpha_1, \alpha_2, \ldots, \alpha_{d-1}]$. The Euclidean distance between $\mathbf{y} \in \partial\mathcal{B}_r(o)$ and $\mathbf{x}_i \triangleq (2l_i, \boldsymbol{\theta}_i) \in \Phi$ is

$$d_2(\mathbf{y}, \mathbf{x}_i) = \sqrt{\sum_{n=1}^{d} (y_n - x_{ni})^2},$$

$$\text{where} \quad x_{ni} = \begin{cases} 2l_i \cos(\theta_{1i}); & n = d, \\ 2l_i \prod_{j=1}^{n} \sin(\theta_{ji}) \cos(\theta_{ni}); & 1 < n < d, \\ 2l_i \prod_{j=1}^{n-1} \sin(\theta_{ji}); & n = d, \end{cases}$$

$$\text{and} \quad y_n = \begin{cases} r \cos(\alpha_1); & n = 1, \\ r \prod_{j=1}^{n} \sin(\alpha_j) \cos(\alpha_n); & n < d, \\ r \prod_{j=1}^{n-1} \sin(\alpha_j); & n = d. \end{cases}$$

It is to be noted that points on $\partial\mathcal{B}_r(o)$ that lie in the typical cell $V_o(\mathcal{C}_\ell^k)$ have to be outside of $\{L_i(r)\}_{i=1}^k$. Now, we define

$$D_i\left(l_i, \boldsymbol{\theta}_i, \mathbf{y}\right) \triangleq \begin{cases} \mathbb{1}\left(d_2(\mathbf{y}, (2l_i, \boldsymbol{\theta}_i)) > r\right); & \text{for } i \in \mathcal{I}(r) \\ 1; & \text{for } i \notin \mathcal{I}(r). \end{cases} \tag{17}$$

Let $\mathbb{D} = [0, 2\pi) \times [0, \pi]^{d-2}$. Using (17), we can now express the portion of $\partial\mathcal{B}_r(o)$ that belongs to the typical cell $V_o(\mathcal{C}_\ell^k)$ as

$$\int_{\mathbb{D}} \prod_{i=1}^{k} D_i\left(l_i, \boldsymbol{\theta}_i, \mathbf{y}\right) \Delta(\boldsymbol{\alpha}) \mathrm{d}\boldsymbol{\alpha} = \frac{1}{r^{d-1}} \upsilon_{d-1}(\partial\mathcal{B}_r(o) \cap V_o(\mathcal{C}_\ell^k)),$$

where $\Delta(\boldsymbol{\alpha}) = \sin^{d-2}(\alpha_1) \times \cdots \times \sin(\alpha_{d-2})$. Note that $\prod_{i=1}^{k} D_i\left(l_i, \boldsymbol{\theta}_i, \mathbf{y}\right)$ is 1 at all points $\mathbf{y}$, such that $0 \leq r \leq z$, lying inside of $\mathcal{B}_z(o) \cap V_o(\mathcal{C}_\ell^k)$, and 0 elsewhere. Thus, the integration of $\prod_{i=1}^{k} D_i\left(l_i, \boldsymbol{\theta}_i, \mathbf{y}\right)$ over all the points $\mathbf{y} \in \mathcal{B}_z(o)$ gives the value of $g_k(z; \mathcal{C}_\ell^k)$ for the given domain configuration, i.e.,

$$g_k(z; \mathcal{C}_\ell^k) = \int_{\mathbb{D}} \int_{r=0}^{z} \prod_{i=1}^{k} D_i\left(l_i, \boldsymbol{\theta}_i, \mathbf{y}\right) r^{d-1} \Delta(\boldsymbol{\alpha}) \mathrm{d}r \mathrm{d}\boldsymbol{\alpha}. \tag{18}$$

Using the above results, we present the distance distribution of a uniformly distributed point in $V_o \cap \mathcal{B}_\ell(o)$ conditioned on $\Phi(\mathcal{B}_{2\ell}(o)) = k$ in the following lemma. In this lemma, we condition on the number of points that form the domain configuration but not on their locations. Let $\mathbf{y}_i = (u_i, \boldsymbol{\alpha}_i)$ and $\tilde{\mathbb{D}}^d = [0, \ell] \times [0, 2\pi) \times [0, \pi]^{d-2}$.

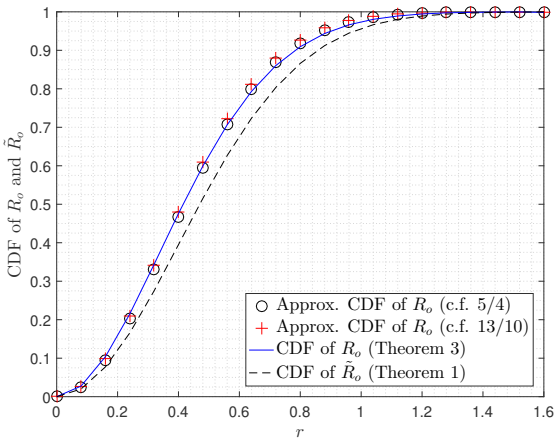

Fig. 4 CDF of R_o and $\tilde{R}_o$ for unit-intensity PPP on $\mathbb{R}^2$.

Lemma 2 *For given ℓ, the CDF of R_ℓ conditioned on $\Phi(\mathcal{B}_{2\ell}(o)) = k$ is*

$$F_{R_\ell}(z;k) = \int\limits_{\left(\tilde{\mathbb{D}}^d\right)^k} \frac{g_k(z;(u_1,\boldsymbol{\alpha}_1),\ldots,(u_k,\boldsymbol{\alpha}_k))}{g_k(\ell;(u_1,\boldsymbol{\alpha}_1),\ldots,(u_k,\boldsymbol{\alpha}_k))} \prod_{i=1}^{k} \frac{1}{\kappa_d \ell^d} u_i^{d-1} \Delta(\boldsymbol{\alpha}_i) \mathrm{d}\mathbf{y}_i. \quad (19)$$

where $g_k(z;(u_1,\boldsymbol{\alpha}_1),\ldots,(u_k,\boldsymbol{\alpha}_k))$ is given by (18).

Proof The CDF of R_ℓ conditioned on $\Phi(\mathcal{B}_{2\ell}(o)) = k$ is $F_{R_\ell}(z;k) = \mathbb{E}_{\mathcal{C}_\ell^k}[F_{R_\ell}(z;\mathcal{C}_\ell^k)]$ where $F_{R_\ell}(z;\mathcal{C}_\ell^k)$ is given by (16), and the pdf of $\mathcal{C}_\ell^k$ is given in (11). □

Using Lemma 2, we obtain the following theorem.

Theorem 3 *For the homogeneous PPP with intensity λ on $\mathbb{R}^d$, the CDF of the distance R_o from the nucleus to a uniformly random point in the typical cell V_o is*

$$F_{R_o}(z) = \lim_{l\to\infty} \sum_{k=0}^{\infty} F_{R_\ell}(z;k)\mathbb{P}(\Phi(\mathcal{B}_{2\ell}(o)) = k), \quad (20)$$

where $F_{R_\ell}(z;k)$ is given in Lemma 2.

Proof We first take the expectation of the conditional CDF of R_ℓ, given in Lemma 2, over k. We then take the limit $\ell \to \infty$ under which this distance distribution of a uniformly distributed point in $V_o \cap \mathcal{B}_\ell(o)$ converges to that of a uniformly distributed point in V_o per (15). □

3.2.4 Numerical Results for $d = 2$

In Fig. 4, we plot the CDF of $\tilde{R}_o$ and the CDF of R_o with $\ell = 1.6$ for $d = 2$. This value for ℓ is selected because the probability that the distance of the farthest point in the typical cell in $\mathbb{R}^2$ is below 1.6 is 0.99 [3]. The integrals in (19) are evaluated numerically using a Monte Carlo integration method. The numerically evaluated mean values of $\tilde{R}_o$ and R_o are 0.500 and 0.445. Given the complicated form of the exact CDF of R_o, it is desirable to construct closed-form approximations that could be used in obtaining design insights in application-oriented studies. On that note, it has been empirically demonstrated in [16] and [22] for $d = 2$ that the CDF of R_o can be tightly approximated by $1 - \exp(-\pi\rho\lambda r^2)$. It is obtained by introducing a correction factor (c.f.) ρ in the CDF of $\tilde{R}_o$ given in (5), which reduces to $1 - \exp(-\pi\lambda r^2)$ for $d = 2$. Furthermore, [16] and [22] empirically show that $\rho = 13/10$ and $5/4$ provide a close match for the exact CDF of R_o. This is also illustrated in Fig. 4. Building on these initial insights, we derive the aforementioned c.f. ρ for the general case of d dimensions in the next section and provide a useful physical interpretation of the resulting value.

4 Approximation of the Distribution of R_o

In this section, we derive the approximate CDF of R_o based on the insight obtained through the empirical results presented in [16] and [22] which are discussed above. In particular, we approximate the CDF of R_o with $1 - \exp(-\rho_d\lambda\kappa_d r^d)$ (i.e., the contact distribution of PPP) where the c.f. ρ_d is determined by matching the d-th derivative of the approximate function with that of the second-order Taylor series expansion of the CDF of R_o at $r = 0$. For this, the moments and covariance of the volume of the typical cell V_o and the volume of the intersection of $\mathcal{B}_r(o)$ with the typical cell V_o are required. Therefore, we now present these intermediate results in the following subsection.

4.1 Some Useful Results

We first present the second moment of the volume of the typical cell V_o in the following lemma.

Lemma 3 *The second moment of the volume of the typical cell V_o is*

$$\mathbb{E}[v_d(V_o)^2] = 4\pi C_{d,2} \int_0^{\pi} \int_0^{\infty} \int_0^{\infty} \exp(-\lambda U(v_1, v_2, u))(v_1 v_2)^{d-1} (\sin u)^{d-2} \mathrm{d}v_2 \mathrm{d}v_1 \mathrm{d}u, \tag{21}$$

where $U(v_1, v_2, u) =$

$$\kappa_d v_1^d + \kappa_d v_2^d - \kappa_d v_1^d \int_0^{\psi_1} \alpha_d \sin^d \psi \mathrm{d}\psi - \kappa_d v_2^d \int_0^{\psi_2} \alpha_d \sin^d \psi \mathrm{d}\psi, \tag{22}$$

$C_{d,2} = \frac{d!}{2(d-2)!}\frac{\kappa_d\kappa_{d-1}}{\kappa_2\kappa_1}$, $\alpha_d = \frac{\Gamma(\frac{d}{2}+1)}{\Gamma(\frac{1}{2})\Gamma(\frac{d+1}{2})}$, $\psi_1 + \psi_2 = \pi - u$ *and* $v_1^d \sin^d \psi_1 = v_2^d \sin^d \psi_2$.

Proof Using [20, Eq. (21)], we obtain the second moment of $\upsilon_d(V_o)$ as

$$\begin{aligned}\mathbb{E}[\upsilon_d(V_o)^2] &= \int_{\mathbb{R}^d}\int_{\mathbb{R}^d} \mathbb{P}(x_1, x_2 \in V_o)\mathrm{d}x_1\mathrm{d}x_2 \\ &= \int_{\mathbb{R}^d}\int_{\mathbb{R}^d} \exp(-\lambda\upsilon_d(\mathcal{B}_{\|x_1\|}(x_1) \cup \mathcal{B}_{\|x_2\|}(x_2)))\mathrm{d}x_2\mathrm{d}x_1. \end{aligned} \tag{23}$$

Next, (21) is obtained using the steps from the proof of [19, Theorem 3.1]. □

The n-th moment of the volume of the intersection of a ball of arbitrary radius with the typical cell is obtained in [19, Lemma 4.2]. Using this result, we present the second moment of $\upsilon_d(\mathcal{B}_r(o) \cap V_o)$ in the following lemma.

Lemma 4 *The second moment of the volume of the intersection of the ball $\mathcal{B}_r(o)$ with the typical cell V_o is* $\mathbb{E}[\upsilon_d(\mathcal{B}_r(o) \cap V_o)^2] =$

$$4\pi C_{d,2}\int_0^\pi\int_0^r\int_0^r \exp(-\lambda U(v_1, v_2, u))(v_1v_2)^{d-1}(\sin u)^{d-2}\mathrm{d}v_2\mathrm{d}v_1\mathrm{d}u, \tag{24}$$

where $U(v_1, v_2, u)$ is given by (22).

In [23, Lemma 3.1], the correlation between the volume of the *typical Stienen ball* and the volume of the typical cell is derived. Using the approach of [23], we provide the covariance of the volumes of $\mathcal{B}_r(o) \cap V_o$ and V_o in the following lemma.

Lemma 5 *The covariance of the volume of the intersection of $\mathcal{B}_r(o)$ with the typical cell V_o and the volume of the typical cell V_o is*

$$\begin{aligned}\mathtt{Cov}[\upsilon_d(\mathcal{B}_r(o) \cap V_o), \upsilon_d(V_o)] &= \frac{1}{2}\mathtt{Var}[\upsilon_d(V_o)] - \frac{1}{2\lambda^2}\left(1 - 2\exp(-\lambda\kappa_d r^d)\right) \\ &+ 2\pi C_{d,2}\int_0^\pi\int_0^r\int_0^r \exp(-\lambda U(v_1, v_2, u))(v_1v_2)^{d-1}(\sin u)^{d-2}\mathrm{d}v_2\mathrm{d}v_1\mathrm{d}u \\ &- 2\pi C_{d,2}\int_0^\pi\int_r^\infty\int_r^\infty \exp(-\lambda U(v_1, v_2, u))(v_1v_2)^{d-1}(\sin u)^{d-2}\mathrm{d}v_2\mathrm{d}v_1\mathrm{d}u, \end{aligned} \tag{25}$$

where $U(v_1, v_2, u)$ is given by (22).

Proof Let $\hat{V}_o(r) = V_o \setminus V_o \cap \mathcal{B}_r(o)$. The variance of the volume of $\hat{V}_o(r)$ is

$$\begin{aligned}\mathtt{Var}[\upsilon_d(\hat{V}_o(r))] &= \mathtt{Var}[\upsilon_d(V_o) - \upsilon_d(\mathcal{B}_r(o) \cap V_o)] \\ &= \mathtt{Var}[\upsilon_d(V_o)] + \mathtt{Var}[\upsilon_d(\mathcal{B}_r(o) \cap V_o)] - 2\mathtt{Cov}[\upsilon_d(\mathcal{B}_r(o) \cap V_o), \upsilon_d(V_o)].\end{aligned}$$

This implies $\mathtt{Cov}[\upsilon_d(\mathcal{B}_r(o) \cap V_o), \upsilon_d(V_o)] =$

$$\frac{1}{2}\mathtt{Var}[\upsilon_d(V_o)] + \frac{1}{2}\mathtt{Var}[\upsilon_d(\mathcal{B}_r(o) \cap V_o)] - \frac{1}{2}\mathtt{Var}[\upsilon_d(\hat{V}_o(r))]. \tag{26}$$

Using Lemmas 1 and 4, the variance of $\upsilon_d(\mathcal{B}_r(o)\cap V_o)$ can be expressed as

$$\mathtt{Var}[\upsilon_d(\mathcal{B}_r(o)\cap V_o)] = 4\pi C_{d,2}\int_0^{\pi}\int_0^{r}\int_0^{r}\exp(-\lambda U(v_1,v_2,u))(v_1v_2)^{d-1}\times (\sin u)^{d-2}\mathrm{d}v_2\mathrm{d}v_1\mathrm{d}u - \frac{1}{\lambda^2}\left(1-\exp(-\lambda\kappa_d r^d)\right)^2. \quad (27)$$

Now, we obtain the mean and variance of $\hat{V}_o(r)$. Using Lemma 1, we get

$$\mathbb{E}[\upsilon_d(\hat{V}_o(r))] = \mathbb{E}[\upsilon_d(V_o) - \upsilon_d(\mathcal{B}_r(o)\cap V_o)] = \frac{1}{\lambda}\exp(-\lambda\kappa_d r^d). \quad (28)$$

Using [20, Eq. (21)], we can obtain the second moment as

$$\begin{aligned}\mathbb{E}[\upsilon_d(\hat{V}_o(r))^2] &= \int_{\mathbb{R}^d}\int_{\mathbb{R}^d}\mathbb{P}(r<\|x_1\|, r<\|x_2\|, x_1,x_2\in V_o(r))\mathrm{d}x_2\mathrm{d}x_1\\ &= \int_{\mathbb{R}^d\setminus\mathcal{B}_r(o)}\int_{\mathbb{R}^d\setminus\mathcal{B}_r(o)}\mathbb{P}(x_1,x_2\in V_o)\mathrm{d}x_2\mathrm{d}x_1\\ &\overset{(a)}{=} 4\pi C_{d,2}\int_0^{\pi}\int_r^{\infty}\int_r^{\infty}\exp(-\lambda U(v_1,v_2,u))(v_1v_2)^{d-1}(\sin u)^{d-2}\mathrm{d}v_2\mathrm{d}v_1\mathrm{d}u, \quad (29)\end{aligned}$$

where (a) follows from the similar steps given in the proof of Lemma 3. Lastly, substituting (27), (28) and (29) in (26) completes the proof. □

Recall, the c.f. ρ_d is determined by matching the d-th derivative of the second-order approximation of the CDF of R_o with that of the approximating function $1-\exp(-\rho_d\lambda\kappa_d r^d)$ at $r=0$. As the second-order Taylor series expansion of the CDF includes the covariance term given in Lemma 5, we first provide its d-th derivative at $r=0$ in the following lemma.

Lemma 6 *The d-th derivative of the covariance of the volume of the intersection of $\mathcal{B}_r(o)$ with the typical cell V_o and the volume of typical cell V_o w.r.t. r is zero at $r=0$.*

Proof Using Lemma 5, we can write

$$\begin{aligned}&\frac{\mathrm{d}^d}{\mathrm{d}r^d}\mathtt{Cov}[\upsilon_d(\mathcal{B}_r(o)\cap V_o),\upsilon_d(V_o)]\Big|_{r=0}\\ &\qquad= \frac{\mathrm{d}^d}{\mathrm{d}r^d}\frac{1}{\lambda^2}\exp(-\lambda\kappa_d r^d)\Big|_{r=0} + \frac{\mathrm{d}^d}{\mathrm{d}r^d}\left(f_1(r)-f_2(r)\right)\Big|_{r=0}, \quad (30)\end{aligned}$$

where

$$f_1(r) = \int_0^r\int_0^r g(v_1,v_2)\mathrm{d}v_2\mathrm{d}v_1, \quad \text{and} \quad f_2(r) = \int_r^{\infty}\int_r^{\infty} g(v_1,v_2)\mathrm{d}v_2\mathrm{d}v_1,$$

such that

$$g(v_1,v_2) = 2\pi C_{d,2}\int_0^{\pi}\exp(-\lambda U(v_1,v_2,u))(v_1v_2)^{d-1}(\sin u)^{d-2}\mathrm{d}u.$$

Further,

$$\frac{\mathrm{d}^d}{\mathrm{d}r^d}\frac{1}{\lambda^2}\exp(-\lambda\kappa_d r^d)\bigg|_{r=0} = -\frac{1}{\lambda}d!\kappa_d = -\frac{1}{\lambda}2\pi^{\frac{d}{2}}\frac{\Gamma(d)}{\Gamma(\frac{d}{2})}. \tag{31}$$

A lengthy but straightforward calculation yields that

$$\frac{\mathrm{d}^d}{\mathrm{d}r^d}\left(f_1(r) - f_2(r)\right)\bigg|_{r=0} = \frac{1}{\lambda}2\pi^{\frac{d}{2}}\frac{\Gamma(d)}{\Gamma(\frac{d}{2})}. \tag{32}$$

Finally, the substitution of (31) and (32) in (30) completes the proof. □

4.2 Approximate CDF of R_o

In the following theorem we determine the c.f. of the approximated CDF of R_o, which is the main result of this section.

Theorem 4 *For the homogeneous PPP with intensity λ on $\mathbb{R}^d$, the approximate CDF of the distance R_o from the nucleus to a uniformly random point in the typical cell V_o is*

$$F_{R_o}(r) \approx 1 - \exp(-\rho_d\lambda\kappa_d r^d), \tag{33}$$

where

$$\rho_d = 1 + \frac{\mathtt{Var}[\upsilon_d(V_o)]}{\mathbb{E}[\upsilon_d(V_o)]^2}. \tag{34}$$

Proof The second order Taylor series expansion of the bivariate function $f(Z_1, Z_2) = \frac{Z_1}{Z_2}$ around the mean $(\bar{z}_1, \bar{z}_2)$ can be written as

$$f(Z_1, Z_2) \approx \frac{\bar{z}_1}{\bar{z}_2} + \frac{1}{\bar{z}_2}(Z_1 - \bar{z}_1) - \frac{\bar{z}_1}{\bar{z}_2^2}(Z_2 - \bar{z}_2) + \frac{1}{\bar{z}_2^2}(Z_1 - \bar{z}_1)(Z_2 - \bar{z}_2) + \frac{\bar{z}_1}{\bar{z}_2^3}(Z_2 - \bar{z}_2)^2.$$

Taking expectation of $f(Z_1, Z_2)$ w.r.t. Z_1 and Z_2, we get

$$\mathbb{E}[f(Z_1, Z_2)] \approx \frac{\bar{z}_1}{\bar{z}_2} - \frac{1}{\bar{z}_2^2}\mathtt{Cov}[z_1, z_2] + \frac{\bar{z}_1}{\bar{z}_2^3}\mathtt{Var}[z_2]. \tag{35}$$

The CDF of R_o is

$$F_{R_o}(r) = \mathbb{E}\left[\frac{\upsilon_d(\mathcal{B}_r(o) \cap V_o)}{\upsilon_d(V_o)}\right].$$

Therefore, using (35), the second-order Taylor series expansion of $F_{R_o}(r)$ around the mean $(\mathbb{E}[\upsilon_d(\mathcal{B}_r(o) \cap V_o)], \mathbb{E}[\upsilon_d(V_o)])$ can be written as $F_{R_o}(r) \approx$

$$\frac{\mathbb{E}[\upsilon_d(\mathcal{B}_r(o) \cap V_o)]}{\mathbb{E}[\upsilon_d(V_o)]}\left[1 + \frac{\mathtt{Var}[\upsilon_d(V_o)]}{\mathbb{E}[\upsilon_d(V_o)]^2}\right] - \frac{\mathtt{Cov}[\upsilon_d(\mathcal{B}_r(o) \cap V_o), \upsilon_d(V_o)]}{\mathbb{E}[\upsilon_d(V_o)]^2}.$$

Using Lemma 3 and Lemma 4, we obtain $F_{R_o}(r) \approx$

$$\left(1-\exp(-\lambda\kappa_d r^d)\right)\left[1+\frac{\mathtt{Var}[\upsilon_d(V_o)]}{\mathbb{E}[\upsilon_d(V_o)]^2}\right]-\frac{\mathtt{Cov}[\upsilon_d(\mathcal{B}_r(o)\cap V_o),\upsilon_d(V_o)]}{\mathbb{E}[\upsilon_d(V_o)]^2}. \quad (36)$$

Now, as $1-\exp(-\rho_d\lambda\kappa_d r^d)$ is considered for the approximation, we determine the c.f. ρ_d by matching the d-th derivatives of $1-\exp(-\rho_d\lambda\kappa_d r^d)$ and $F_{R_o}(r)$ at $r=0$ as

$$\rho_d=\frac{1}{d!\lambda\kappa_d}\frac{\mathrm{d}^d}{\mathrm{d}r^d}F_{R_o}(r)\bigg|_{r=0}.$$

Therefore, using (36) and Lemma 6 we have

$$\rho_d=1+\frac{\mathtt{Var}[\upsilon_d(V_o)]}{\mathbb{E}[\upsilon_d(V_o)]^2}.$$

This completes the proof. □

Before giving the numerical validation of the approximated CDF of R_o, we present the approximated n-th moment of the distance R_o and some useful observations about the c.f. in the following corollaries.

Corollary 1 *For the homogeneous PPP with intensity λ on $\mathbb{R}^d$, the n-th moments of the distances $\tilde{R}_o$ and R_o from the nucleus to a uniformly random point in the 0-cell and typical cell are, respectively, given by*

$$\mathbb{E}[\tilde{R}_o^n]=\frac{\Gamma\left(1+\frac{n}{d}\right)}{(\lambda\kappa_d)^{\frac{n}{d}}} \quad \textit{and} \quad \mathbb{E}[R_o^n]\approx\frac{\Gamma\left(1+\frac{n}{d}\right)}{(\rho_d\lambda\kappa_d)^{\frac{n}{d}}}. \quad (37)$$

Proof The expressions for $\mathbb{E}[\tilde{R}_o^n]$ and $\mathbb{E}[R_o^n]$ directly follow from Theorems 1 and 4, respectively. □

Corollary 2 *For the homogeneous PPP with intensity λ on $\mathbb{R}^d$, the CDF of the distance R_o from the nucleus to a uniformly random point in the typical cell V_o can be approximated as $1-\exp(-\lambda\kappa_d\rho_d r^d)$ where*

$$\rho_d=\frac{\mathbb{E}[\upsilon_d(\tilde{V}_o)]}{\mathbb{E}[\upsilon_d(V_o)]}. \quad (38)$$

Proof From [7, Equation 2.5], we have

$$\mathbb{E}[\upsilon_d(\tilde{V}_o)]=\mathbb{E}[\upsilon_d(V_o)]+\frac{\mathtt{Var}[\upsilon_d(V_o)]}{\mathbb{E}[\upsilon_d(V_o)]}.$$

Substituting the above expression in (34) gives (38). □

Corollary 3 $\lim\limits_{d\to\infty}\rho_d=1$.

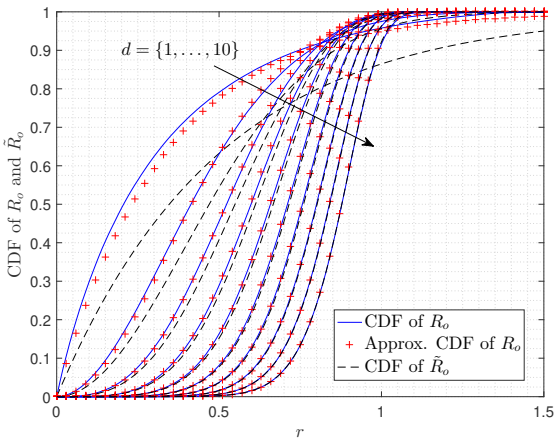

Fig. 5 CDF of R_o and $\tilde{R}_o$ for unit-intensity PPP on $\mathbb{R}^d$ where $d \in \{1, \ldots, 10\}$. The CDF of $\tilde{R}_o$ and approximate CDF of R_o are given in Theorem 1 and Theorem 4, respectively.

Proof Using [19, Theorem 3.1], we can write

$$\lim_{d\to\infty} \mathtt{Var}[\upsilon_d(V_o)] = 0.$$

Since, the mean volume of the PV cell is λ^{-1} for any d, the proof directly follows using (34) and above result. □

Remark 2 From (37), it is clear that the ratio of the means of $\tilde{R}_o$ and R_o is approximately $\sqrt[d]{\rho_d}$. Therefore, using Corollary 2, we can infer that the ratio of the means of $\tilde{R}_o$ and R_o is approximately equal to the d-th root of the ratio of the mean volumes of the 0-cell $\tilde{V}_o$ and the typical cell V_o. In other words, the distance from the nucleus to a uniformly random point in the typical cell scales with the distance from the nucleus to a uniformly random point in the 0-cell by a factor equal to the d-th root of the ratio of the mean volumes of the 0-cell $\tilde{V}_o$ and the typical cell V_o.

4.3 Numerical Comparisons

For the numerical evaluation of the approximated CDF of R_o, we obtain the c.f. ρ_d using (34) for which the mean and variance of the volume of the typical cell are evaluated using Lemma 3. Fig. 5 validates the accuracy of the approximated CDF of R_o by comparing it with the Monte Carlo simulations for the cases of $d \in \{1, \ldots, 10\}$. Fig. 5 clearly indicates that the CDF of R_o gradually approaches that of $\tilde{R}_o$ as d increases. Further, Table 1 verifies the accuracy of the approximated mean and variance of R_o (obtained using Corollary 1) for $d \in \{1, \ldots, 10\}$. For $d = 2$, the obtained mean value of R_o is 0.442 which is also close to the mean values 0.438 and 0.447 obtained using the curve-fitted c.f.s $13/10$ and $5/4$ of [16] and [22], respectively.

Table 1 Accuracy of Approximated Mean and Variance of R_o.

d		1	2	3	4	5	6	7	8	9	10
ρ_d		1.500	1.285	1.171	1.128	1.079	1.062	1.043	1.032	1.029	1.018
$\mathbb{E}[R_o]$	Exact	0.305	0.445	0.529	0.595	0.651	0.701	0.749	0.798	0.831	0.873
	Approx.	0.333	0.442	0.524	0.591	0.648	0.698	0.745	0.789	0.829	0.862
$\mathtt{Var}[R_o]$	Exact	0.090	0.058	0.038	0.028	0.022	0.019	0.016	0.014	0.013	0.012
	Approx.	0.111	0.053	0.036	0.028	0.022	0.018	0.015	0.013	0.012	0.011

5 Limiting Shape of Large PV Cells

Thus far, we have presented an exact characterization of the CDFs of $\tilde{R}_o$ and R_o in Sections 2 and 3 and a closed-form approximation for the multi-integral exact expression for the CDF of R_o in Section 4. It is worth noting that the conditioning on the k points of Φ in the $\mathcal{B}_{2\ell}(o)$, defined as the domain configuration $\mathcal{C}_\ell^k$ (see (10)), allowed us to construct the set of surfaces of the spherical caps $\{L_i(\ell)\}_{i=1}^k$ on the ball $\mathcal{B}_\ell(o)$ as in (13). This helps in determining the conditional volume of the typical cell V_o and thus the conditional CDF of R_o. It is easy to observe that some points of the domain configuration $\mathcal{C}_\ell^k$ are the closest points on some boundaries of the typical cell V_o and thus the lines joining them to origin are perpendicular to the corresponding boundaries. Further, these points are also the midpoints of the chords formed by the corresponding spherical caps. This implies that these surfaces of spherical caps completely lie outside the typical cell V_o (see Fig. 2 for $d = 2$). Therefore, it is quite straightforward to see that the typical cell is completely contained within $\mathcal{B}_\ell(o)$ only if the set $\{L_i(\ell)\}_{i=1}^k$ completely covers the boundary of $\mathcal{B}_\ell(o)$. Using this fact, in this section, we provide an alternate proof to the well-known spherical property of d-dimensional PV cells containing a large inball.

Let the point $\tilde{\mathbf{x}}_0 \triangleq (R, \boldsymbol{\theta}_0)$ denote the nearest point on the boundary of the typical cell V_o to its nucleus. Therefore, R is the radius of the largest ball $\mathcal{B}_R(o)$ contained within the typical cell V_o, henceforth called the inradius of the cell. In this construction, it is evident that the nearest point $\mathbf{x}_0$ in Φ from the nucleus of V_o (i.e., the origin) is at $(2R, \boldsymbol{\theta}_0)$ such that $\|\tilde{\mathbf{x}}_0\| = \frac{1}{2}\|\mathbf{x}_0\| = R$. Note that the results presented in the following are conditioned on the inradius R.

Let $\mathcal{A}(r, \epsilon)$ denote the annulus formed by two balls of radii r and $r + \epsilon$ co-centered at the origin. Now, consider the domain configuration $\mathcal{C}_R^k = \{\tilde{\mathbf{x}}_i\}_{i=1}^k$ as the set containing the mid-point of lines joining the nucleus of V_o and the points in $\Phi \cap \mathcal{A}(2R, 2\epsilon)$ given $\Phi(\mathcal{A}(2R, 2\epsilon)) = k$. Fig. 6 illustrates a potential configuration of $\mathcal{C}_R^2$ for the case of $d = 2$. By the Poisson property, the k points of $\mathcal{C}_R^k$ are distributed uniformly at random independently of each other in the annulus $\mathcal{A}(R, \epsilon)$ such that the CDF of $\|\tilde{\mathbf{x}}_i\| = l_i$, for $\forall i$, conditioned on R is

$$F_{l_i}(l) = \frac{l^d - R^d}{(R+\epsilon)^d - R^d}, \quad R \le l \le R + \epsilon. \tag{39}$$

We define the set of $k + 1$ spherical caps $\{L_i(R + \epsilon)\}_{i=0}^k$ corresponding to points $\{\tilde{\mathbf{x}}\}_{i=0}^k = \{\tilde{\mathbf{x}}_0 \cup \mathcal{C}_R^k\}$ on the $\mathcal{B}_{R+\epsilon}(o)$ with heights equal to ϵ for $i = 0$

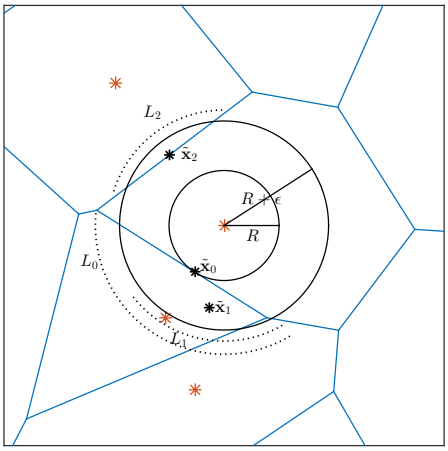

Fig. 6 Typical cell with inradius R for the case of $d = 2$.

and $R+\epsilon-l_i$ for $i = 1, \ldots, k$. The surface area of the spherical cap $L_i(R+\epsilon)$ is [24]

$$S_i = \begin{cases} \frac{1}{2}\chi_d (R+\epsilon)^{d-1} I_{1-\frac{R^2}{(R+\epsilon)^2}} \left(\frac{d-1}{2}, \frac{1}{2}\right), & \text{for } i = 0 \\ \frac{1}{2}\chi_d (R+\epsilon)^{d-1} I_{1-\frac{l_i^2}{(R+\epsilon)^2}} \left(\frac{d-1}{2}, \frac{1}{2}\right), & \text{for } i = 1, \ldots, k, \end{cases} \tag{40}$$

where $\chi_d = \frac{2\pi^{\frac{d}{2}}}{\Gamma(\frac{d}{2})}$ is the surface area of the unit radius ball in $\mathbb{R}^d$ and $I_z(a,b) = \frac{B_z(a,b)}{B(a,b)}$ such that $B(a,b)$ and $B_z(a,b)$ are the beta function and the incomplete beta function, respectively. Note that $0 \leq S_i \leq S_0 \ \forall i$. Since the points in $\mathcal{C}_R^k$ are i.i.d. in $\mathcal{A}(R,\epsilon)$, the spherical caps $\{L_i(R+\epsilon)\}_{i=1}^k$ of i.i.d. surface areas are placed uniformly at random independently of each other on $\mathcal{B}_{R+\epsilon}(o)$.

Now, we evaluate the probability that the uniformly chosen point $(R+\epsilon, \boldsymbol{\alpha})$ on the surface of $\mathcal{B}_{R+\epsilon}(o)$ belongs to the spherical cap $L_i(R+\epsilon)$, for $i \in \{1, \ldots, k\}$, as

$$\begin{aligned} p &= \mathbb{P}((R+\epsilon, \boldsymbol{\alpha}) \text{ belongs to the cap } L_i(R+\epsilon) \text{ of area } S_i) \\ &= \frac{1}{\chi_d (R+\epsilon)^{d-1}} \mathbb{E}[S_i] \\ &\overset{(a)}{=} d\tilde{\nu}_R \int_R^{R+\epsilon} I_{1-\frac{l^2}{(R+\epsilon)^2}} \left(\frac{d-1}{2}, \frac{1}{2}\right) l^{d-1} \mathrm{d}l \\ &\overset{(b)}{=} \frac{\tilde{\nu}_R (R+\epsilon)^d}{B\left(\frac{d-1}{2}, \frac{1}{2}\right)} B_{1-\frac{R^2}{(R+\epsilon)^2}} \left(\frac{d-1}{2}, \frac{d+1}{2}\right) - \tilde{\nu}_R R^d I_{1-\frac{R^2}{(R+\epsilon)^2}} \left(\frac{d-1}{2}, \frac{1}{2}\right), \end{aligned} \tag{41}$$

where $\tilde{\nu}_R = \frac{1}{2((R+\epsilon)^d - R^d)}$. Step (a) follows using the pdf of l_i which is obtained using (39) and (b) follows using the steps given in Appendix A. Also note that

the probability that the uniformly chosen point $(R+\epsilon, \boldsymbol{\alpha})$ on the surface of $\mathcal{B}_{R+\epsilon}(o)$ belongs to the spherical cap $L_0(R+\epsilon)$ is

$$p_0 = \frac{1}{2} I_{1-\frac{R^2}{(R+\epsilon)^2}} \left(\frac{d-1}{2}, \frac{1}{2} \right). \tag{42}$$

Let $K = \Phi\left(\mathcal{A}(2R, 2\epsilon)\right)$. By definition, K is Poisson with mean $\lambda\kappa_d((R+\epsilon)^d - R^d)$. Now to complete our argument, we evaluate the probability that the point on the boundary of $\mathcal{B}_{R+\epsilon}(o)$ does not belong to V_o as

$$\begin{aligned} Q_d(R,\epsilon) &= \mathbb{P}((R+\epsilon, \boldsymbol{\alpha}) \text{ belongs to at least one of the caps}) \\ &= 1 - (1-p_0)\mathbb{E}\left[(1-p)^K\right] \\ &\overset{(a)}{=} 1 - \left(1 - \frac{1}{2} I_{1-\frac{R^2}{(R+\epsilon)^2}} \left(\frac{d-1}{2}, \frac{1}{2} \right)\right) \exp\left(-\frac{1}{2}\lambda\kappa_d h(R,\epsilon) \right), \end{aligned} \tag{43}$$

where $h(R,\epsilon) = \frac{(R+\epsilon)^d}{B\left(\frac{d-1}{2}, \frac{1}{2}\right)} B_{1-\frac{R^2}{(R+\epsilon)^2}}\left(\frac{d-1}{2}, \frac{d+1}{2}\right) - R^d I_{1-\frac{R^2}{(R+\epsilon)^2}}\left(\frac{d-1}{2}, \frac{1}{2}\right)$, and (a) directly follows using (41), (42) and the probability generating function of the Poisson distribution with mean $\lambda\kappa_d((R+\epsilon)^d - R^d)$. Now, in the following theorem we state the limiting case of (43).

Theorem 5

$$\lim_{R\to\infty} Q_d(R,\epsilon) = 1, \qquad \forall \epsilon > 0. \tag{44}$$

Proof We note that, for $\epsilon > 0$, $I_{1-\frac{R^2}{(R+\epsilon)^2}}\left(\frac{d-1}{2}, \frac{1}{2}\right) \to 0$ as $R \to \infty$. Therefore, in order to prove (44), it is sufficient to show that the exponential term in (43) tends to 0 as $R \to \infty$ for $\epsilon > 0$, i.e.,

$$\lim_{R\to\infty} h(R,\epsilon) = \infty.$$

To this end, we multiply $h(R,\epsilon)$ with $B\left(\frac{d-1}{2}, \frac{1}{2}\right)$ to obtain $\tilde{h}(R,\epsilon) =$

$$(R+\epsilon)^d B_{1-\frac{R^2}{(R+\epsilon)^2}}\left(\frac{d-1}{2}, \frac{d+1}{2}\right) - R^d B_{1-\frac{R^2}{(R+\epsilon)^2}}\left(\frac{d-1}{2}, \frac{1}{2}\right). \tag{45}$$

We have

$$B_{1-\frac{R^2}{(R+\epsilon)^2}}\left(\frac{d-1}{2}, a\right) = \int_0^{1-\frac{R^2}{(R+\epsilon)^2}} t^{\frac{d-1}{2}-1}(1-t)^{a-1}\mathrm{d}t.$$

Thus, using the binomial expansion of the term $(1-t)^{a-1}$, we get

$$\begin{aligned} B_{1-\frac{R^2}{(R+\epsilon)^2}}\left(\frac{d-1}{2}, a\right) &= \int_0^{1-\frac{R^2}{(R+\epsilon)^2}} t^{\frac{d-1}{2}-1} \sum_{k=0}^{\infty}(-1)^k \frac{1}{k!} \prod_{l=0}^{k-1}(a-1-l) t^k \mathrm{d}t \\ &= \sum_{k=0}^{\infty}(-1)^k \frac{1}{k!} \prod_{l=0}^{k-1}(a-1-l) \int_0^{1-\frac{R^2}{(R+\epsilon)^2}} t^{k+\frac{d-1}{2}-1}\mathrm{d}t \end{aligned}$$

$$= \sum_{k=0}^{\infty} (-1)^k \frac{\prod_{l=0}^{k-1}(a-1-l)}{k!\left(k+\frac{d-1}{2}\right)} \left(1-\frac{R^2}{(R+\epsilon)^2}\right)^{k+\frac{d-1}{2}}.$$

Let $A_k = \frac{1}{k!(k+\frac{d-1}{2})} \prod_{l=0}^{k-1} \left(\frac{d+1}{2}-1-l\right)$ and $B_k = \frac{1}{k!(k+\frac{d-1}{2})} \prod_{l=0}^{k-1} \left(\frac{1}{2}-1-l\right)$. Using the above expansion, we can rewrite (45) as

$$\begin{aligned}
\tilde{h}(R,\epsilon) &= \sum_{k=0}^{\infty} (-1)^k \left[A_k (R+\epsilon)^d - B_k R^d\right] \left(1-\frac{R^2}{(R+\epsilon)^2}\right)^{k+\frac{d-1}{2}} \\
&= \sum_{k=0}^{\infty} (-1)^k \left[(A_k - B_k) R^d + A_k \sum_{n=0}^{d-1} \binom{d}{n} R^n \epsilon^{d-n}\right] \frac{(2R\epsilon+\epsilon^2)^{k+\frac{d-1}{2}}}{(R+\epsilon)^{2k+d-1}} \\
&= \sum_{k=0}^{\infty} (-1)^k \left[(A_k - B_k) R^{\frac{d+1}{2}-k} + A_k \sum_{n=0}^{d-1} \binom{d}{n} R^{n+\frac{1-d}{2}-k} \epsilon^{d-n}\right] \\
&\qquad \times \frac{(2\epsilon + R^{-1}\epsilon^2)^{k+\frac{d-1}{2}}}{(1+R^{-1}\epsilon)^{2k+d-1}}.
\end{aligned}$$

Now note that $A_k - B_k \geq 0$ for $k \leq \frac{d-1}{2}$. Therefore, the terms in the above summation tend to infinity as R tends to infinity for $k < \frac{d+1}{2}$. In addition, the terms converge to a constant for $k = \frac{d+1}{2}$ (if d is odd) and to zero for $k > \frac{d+1}{2}$. From this, it is clear that $\tilde{h}(R,\epsilon) \to \infty$ as $R \to \infty$. Therefore, we have $h(R,\epsilon) \to \infty$ as $R \to \infty$. □

From Theorem 5, it is easy to see that the boundary of a PV cell V_o must be contained within the annulus $\mathcal{A}(R,\epsilon)$ as its inradius $R \to \infty$ for an arbitrarily small ϵ. Hence PV cells with large inradii tend to be spherical. Therefore, the approach presented in this section provides an alternate proof for the well-known *spherical* nature of the PV cells having a large inball [3, 25, 26]. A realization of a PV cell V_o with large inradius is shown in Fig. 7 for $d = 2$.

A Solution of Integral in (41)

Let $a = \frac{d-1}{2}$ and $b = \frac{1}{2}$. From step (a) of (41) and using $I_x(a,b) = \frac{B_x(a,b)}{B(a,b)}$, we have

$$p = \nu_R \int_R^{R+\epsilon} B_{1-\frac{l^2}{(R+\epsilon)^2}}(a,b)\, l^{d-1} \mathrm{d}l,$$

where $\nu_R = \frac{d((R+\epsilon)^d - R^d)^{-1}}{2B(a,b)}$. We solve the above integral using integration by parts as follows. Let $v = l^{d-1}$ and $u = B_{1-\frac{l^2}{(R+\epsilon)^2}}\left(\frac{d-1}{2}, \frac{1}{2}\right)$. We have

$$\frac{\mathrm{d}}{\mathrm{d}l} u = -\frac{2l}{(R+\epsilon)^2} \left(\frac{l^2}{(R+\epsilon)^{2)}}\right)^{b-1} \left(1-\frac{l^2}{(R+\epsilon)^2}\right)^{a-1},$$

and thus

$$p = -\nu_R \frac{R^d}{d} B_{1-\frac{R^2}{(R+\epsilon)^2}}(a,b) + \nu_R \int_R^{R+\epsilon} \frac{l^d}{d} \frac{2l}{(R+\epsilon)^2} \frac{l^{2(b-1)}}{(R+\epsilon)^{2(b-1)}} \left(1-\frac{l^2}{(R+\epsilon)^2}\right)^{a-1} \mathrm{d}l.$$

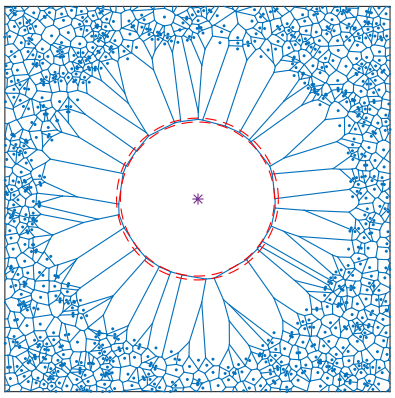

Fig. 7 Illustration of a cell in $\mathbb{R}^2$ with large inradius.

Now, substituting $\frac{l^2}{(R+\epsilon)^2} = z$, we get

$$
\begin{aligned}
p &= -\nu_R \frac{R^d}{d} B_{1-\frac{R^2}{(R+\epsilon)^2}}(a,b) + \nu_R \frac{(R+\epsilon)^d}{d} \int_{\frac{R^2}{(R+\epsilon)^2}}^{1} z^{b+\frac{d}{2}-1}(1-z)^{a-1}\mathrm{d}z \\
&= -\nu_R \frac{R^d}{d} B_{1-\frac{R^2}{(R+\epsilon)^2}}(a,b) + \nu_R \frac{(R+\epsilon)^d}{d} \left[B\left(b+\frac{d}{2}-1,a\right) - B_{\frac{R^2}{(R+\epsilon)^2}}\left(b+\frac{d}{2}-1,a\right)\right] \\
&= -\tilde{\nu}_R R^d I_{1-\frac{R^2}{(R+\epsilon)^2}}(a,b) + \tilde{\nu}_R (R+\epsilon)^d \frac{B\left(b+\frac{d}{2},a\right)}{B(a,b)} \left[1 - I_{1-\frac{R^2}{(R+\epsilon)^2}}\left(b+\frac{d}{2},a\right)\right] \\
&\overset{(a)}{=} \tilde{\nu}_R (R+\epsilon)^d B_{1-\frac{R^2}{(R+\epsilon)^2}}\left(a,b+\frac{d}{2}\right) - \tilde{\nu}_R R^d I_{1-\frac{R^2}{(R+\epsilon)^2}}(a,b)
\end{aligned}
$$

where $\tilde{\nu}_R = \frac{1}{2((R+\epsilon)^d - R^d)}$. Step (a) follows using $I_x(a,b) = 1 - I_{1-x}(b,a)$ and $B(a,b) = B(b,a)$.

Acknowledgements

This work was supported by the United States National Science Foundation under Grant ECCS-1731711.

References

1. J. Møller, "Random tessellations in $\mathbb{R}^d$," *Advances in Applied Probability*, vol. 21, no. 1, pp. 37–73, 1989.
2. L. Muche and D. Stoyan, "Contact and chord length distributions of the Poisson Voronoi tessellation," *Journal of Applied Probability*, vol. 29, no. 2, pp. 467–471, 1992.
3. P. Calka, "The distributions of the smallest disks containing the Poisson-Voronoi typical cell and the Crofton cell in the plane," *Advances in Applied Probability*, vol. 34, no. 4, pp. 702–717, 2002.
4. ——, "An explicit expression for the distribution of the number of sides of the typical Poisson-Voronoi cell," *Advances in Applied Probability*, vol. 35, no. 4, pp. 863–870, 2003.

5. D. Hug, M. Reitzner, and R. Schneider, "Large Poisson-Voronoi cells and Crofton cells," *Advances in Applied Probability*, vol. 36, no. 3, pp. 667–690, 2004.
6. S. Kumar, S. K. Kurtz, J. R. Banavar, and M. Sharma, "Properties of a three-dimensional Poisson-Voronoi tesselation: A Monte Carlo study," *Journal of Statistical Physics*, vol. 67, no. 3-4, pp. 523–551, 1992.
7. J. Mecke, "On the relationship between the 0-cell and the typical cell of a stationary random tessellation," *Pattern Recognition*, vol. 32, no. 9, pp. 1645 – 1648, 1999.
8. K. Koufos and C. P. Dettmann, "Distribution of cell area in bounded Poisson Voronoi tessellations with application to secure local connectivity," *Journal of Statistical Physics*, vol. 176, pp. 1296–1315, 2019.
9. B. Jahnel and A. Tóbiás, "Exponential moments for planar tessellations," *Journal of Statistical Physics*, pp. 1–20, 2020.
10. E. Pineda and D. Crespo, "Temporal evolution of the domain structure in a Poisson-Voronoi transformation," *Journal of Statistical Mechanics: Theory and Experiment*, vol. 2007, no. 06, p. P06007, 2007.
11. F. Baccelli and B. Blaszczyszyn, "Stochastic geometry and wireless networks: volume I theory," *Foundations and Trends in Networking*, 2009.
12. J. G. Andrews, F. Baccelli, and R. K. Ganti, "A tractable approach to coverage and rate in cellular networks," *IEEE Transactions on Communications*, vol. 59, no. 11, pp. 3122–3134, Nov. 2011.
13. H. S. Dhillon, R. K. Ganti, F. Baccelli, and J. G. Andrews, "Modeling and analysis of K-tier downlink heterogeneous cellular networks," *IEEE Journal on Selected Areas in Communications*, vol. 30, no. 3, pp. 550 – 560, Apr. 2012.
14. M. Haenggi, *Stochastic Geometry for Wireless Networks*. Cambridge University Press, 2013.
15. B. Blaszczyszyn, M. Haenggi, P. Keeler, and S. Mukherjee, *Stochastic Geometry Analysis of Cellular Networks*. Cambridge University Press, 2018.
16. M. Haenggi, "User point processes in cellular networks," *IEEE Wireless Communications Letters*, vol. 6, no. 2, pp. 258–261, April 2017.
17. P. D. Mankar, P. Parida, H. S. Dhillon, and M. Haenggi, "Downlink analysis for the typical cell in Poisson cellular networks," *IEEE Wireless Communications Letters*, vol. 9, no. 3, pp. 336–339, 2020.
18. J. Møller, *Lectures on random Voronoi tessellations*. Springer Science & Business Media, 2012, vol. 87.
19. K. Alishahi and M. Sharifitabar, "Volume degeneracy of the typical cell and the chord length distribution for Poisson-Voronoi tessellations in high dimensions," *Advances in Applied Probability*, vol. 40, no. 4, pp. 919–938, 12 2008.
20. H. E. Robbins, "On the measure of a random set," *The Annals of Mathematical Statistics*, vol. 15, no. 1, pp. 70–74, 03 1944.
21. E. Pineda and D. Crespo, "Temporal evolution of the domain structure in a Poisson-Voronoi nucleation and growth transformation: Results for one and three dimensions," *Physical Review E*, vol. 78, no. 2, p. 021110, 2008.
22. Y. Wang, M. Haenggi, and Z. Tan, "The meta distribution of the SIR for cellular networks with power control," *IEEE Transactions on Communications*, vol. 66, no. 4, pp. 1745–1757, April 2018.
23. V. Olsbo, "On the correlation between the volumes of the typical Poisson Voronoi cell and the typical Stienen sphere," *Advances in Applied Probability*, vol. 39, no. 4, pp. 883–892, 2007.
24. S. Li, "Concise formulas for the area and volume of a hyperspherical cap," *Asian Journal of Mathematics and Statistics*, vol. 4, no. 1, pp. 66–70, 2011.
25. P. Calka and T. Schreiber, "Limit theorems for the typical Poisson–Voronoi cell and the Crofton cell with a large inradius," *The Annals of Probability*, vol. 33, no. 4, pp. 1625–1642, 2005.
26. R. E. Miles, "A heuristic proof of a long-standing conjecture of D. G. Kendall concerning the shapes of certain large random polygons," *Advances in Applied Probability*, vol. 27, no. 2, pp. 397–417, 1995.